



Flow Characteristics of the Liquid Film During Centrifugal Granulation of Liquid Slag on the Surface of Rotary Cup

Ningwen Xu¹ · Jun Zhao¹ · Xi Zhang² · Meiquan Li² · Chen Ma³ · Zhiqiang Wu³ · Haiyu Meng³ · Shuzhong Wang¹

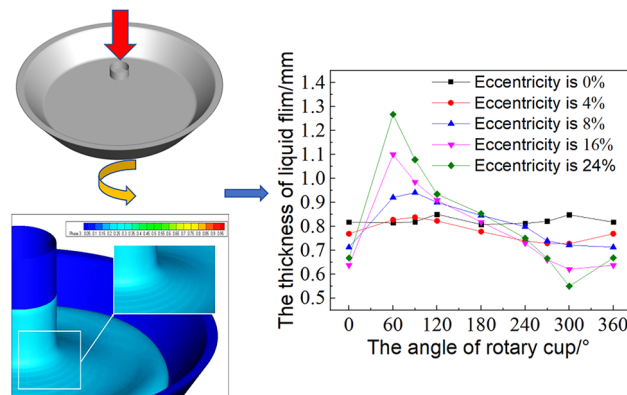
Received: 25 April 2021 / Accepted: 6 September 2021 / Published online: 4 March 2022
© The Minerals, Metals & Materials Society 2022

Abstract

In the process of recovering waste heat from molten slag by dry centrifugal granulation, the particle size and morphology of granulated particles are closely related to the liquid film flow characteristics on the surface of the rotary cup. This paper adopts the numerical simulation method to analyze the spreading characteristics of the liquid film on the surface of the rotary cup under the different conditions of the operating parameters, structural parameters of the rotary cup, the modes of slag inlet tube and rotary cup coordination, and the eccentricity, respectively. The results obtained show that when the rotation speed was increased, the thickness of the liquid film on the inclined wall of the rotary cup decreased, and the decreasing trend gradually decreased. When the flow rate of slag was increased by 50%, the liquid film thickness was increased by about 44%, which changed approximately linearly. Moreover, as the initial temperature of the slag decreased, the spreading of liquid film thickened on the surface of the rotary cup. It was also found that the 30°–60° rotary cup inclination angle was beneficial to thin the liquid film. The slag tube diameter/rotator diameter and the dropping height of slag only affected the liquid film thickness near the center of the rotary cup. The slag eccentricity caused the liquid film to appear in the thickened area and thinned area. Finally, a liquid film thickness correlation at the edge of the rotary cup was obtained to predict the liquid film thickness.

Graphical Abstract

The picture shows the process of the liquid slag entering and spreading on the rotor surface. This paper mainly introduced some regular information affected by operation parameters, structural parameters, and unstable working conditions.



Keywords Liquid slag · Centrifugal granulation · Flow characteristics · Liquid film

Ningwen Xu and Jun Zhao have contributed equally to this work and should be considered co-first authors.

The contributing editor for this article was Sharif Jahanshahi.

Extended author information available on the last page of the article

List of Symbols

- a Fitting constants
- b Fitting constants
- c Fitting constants
- d Fitting constants

e	Fitting constants
E	Energy (J/kg)
Ek	Ekman number
F_{SF}	Body force (N/m ³)
F_{vol}	Surface force (N/m ³)
g	Acceleration of gravity (m/s ²)
h_N	Theoretical film thickness (m)
H	The depth of the rotary cup (m)
k_{eff}	Effective diffusion coefficient (W/(m K))
p	Pressure (Pa)
q	Subscript for a Phase
Q	Volumetric flow (m ³ /s)
Q_m	The mass flow rate (kg/s)
Q^+	The non-dimensional flow rate
R	The radius of the rotary cup (m)
Re	Reynolds number
S_h	Source term (W/m ³)
T	Temperature (K)
$T_{liquidus}$	Solidification temperature of material (K)
$T_{solidus}$	Melting temperature of material (K)
t	Time (s)
u	Speed in x direction (m/s)
\mathbf{u}	Velocity vector in x direction (m/s)
v	Speed in y direction (m/s)
\mathbf{V}	Velocity vector in y direction (m/s)
w	Speed in z direction (m/s)
We	Weber number

Greek Symbols

α_q	The volume fraction
β	The liquid ratio
κ	Local curvature of free surface (1/m)
ρ	Density (kg/m ³)
σ	Surface tension (N/m)
ω	Rotary speed (rad/s)
μ	Dynamic viscosity (Pa s)
μ_{eff}	Effective dynamic viscosity (Pa s)
δ	The thickness of liquid film (m)
ψ	The dip angle of the inner wall surface (°)

Introduction

Molten slag is one of the few undeveloped waste heat resources in the iron and steel industry. Because its discharge temperature is as high as about 1450° C and each ton of slag contains about 1700 MJ of heat, which is equivalent to the heating value of 0.058t standard coal [1]. The sensible heat of molten slag could be recovered as a high-grade waste heat resource and has a high recovery value [2, 3]. Chinese annual production of molten slag is about 300 million tons, with a contained sensible heat being close to combustion of 23 million tons of standard coal. The potential energy-saving

and reduction in emission are huge. Thus it is necessary to adopt technology to recover the remaining heat [4]. Scholars have studied many slag waste heat recovery technologies, including wind quenching granulation technology [5], drum granulation technology [6], Merotec technology [2, 7], mechanical stirring granulation technology [5], continuous casting and rolling technology [5], chemical method [8–10], and dry centrifugal granulation technology [11–14]. Among the many proposed molten slag waste heat recovery technologies, dry centrifugal granulation technology has received the interest and attention of several scholars in China and abroad because of the advantages of uniform slag particle size, high glass content, high waste heat recovery efficiency, and environmental friendliness [15, 16].

The utilization of dry centrifugal granulation technology to recover slag waste heat was first proposed by Pickering [12]. After that, the centrifugal granulation technology had been extensively studied by many scholars. The general process of the dry centrifugal granulation process is molten liquid slag is delivered through a slag pipe to high-speed spinning discs or cups and is rapidly broken into droplets under the disturbance of centrifugal force, surface tension, and unstable waves. At present, the technology has been in the pilot stage, but there are still some problems, such as low waste heat recovery efficiency and slag wool production [17]. The particle size is important factor for heat transfer and heat recovery. The particle size was too large, which caused problems such as slow cooling rate and low waste heat recovery efficiency. The size of the granulated particles is closely related to the spreading characteristics of the liquid film on the surface of the granulator, especially the thickness of the liquid film on the edge of the discs or cups directly determines the particle size [3, 18]. Studying the influence of the spreading characteristics of the liquid film on the granulator surface is very important for controlling the particle size.

First of all, the scholars conducted a preliminary study on the prediction model of liquid film flow and the influence factors of liquid film thickness. Emslie et al. [19] studied the liquid film flow on the surface of the rotating discs. They believed that the change of the liquid film speed on the surface of the disc was mainly controlled by the centrifugal force and proposed a centrifugal model. However, this model was only applicable to the liquid film flow with a large Ekman number, and the predicted liquid film thickness is too large. At the same time, Charwat [20] and Rauscher et al. [21] also obtained an empirical model of liquid film thickness prediction at the edge of the disc through experimental research and dimensional analysis. Later, Zhao et al. [22, 23] proposed a model for calculating the thickness and velocity of the liquid film of the spinning cup under the fully developed flow. Based on the theory of lubrication, Myers and Charpin et al. [24] studied the effect of Coriolis force

on the liquid film formation on the rotating disc and found that when the flow was axisymmetric, the Coriolis force had almost no effect on the thickness of the liquid film.

With the development of computers, CFD numerical simulation has become an essential tool for studying the spreading characteristics of liquid films under centrifugal granulation. Pan et al. [25–28] in CRISO simulated the flow characteristics of liquid film on the disc during the centrifugal granulation process of slag for several years and achieved significant research results. At the same time, other scholars also established numerical models to study the thickness of liquid films. Purwanto et al. [13] found a CFD model of the liquid flow on the surface of the rotating disc to show the thickness of the liquid film at the edge of the disk. Chang et al. [29] studied the flow and granulation characteristics of the molten slag on smooth and non-smooth rotating discs experimentally and numerically. They pointed out that smooth surfaces are more likely to obtain small-size particles and avoid filaments. Wang et al. [30–32] established a two-dimensional numerical model of molten slag–air two-phase flow based on the fluid volume function method (VOF) during the centrifugal granulation of rotating disc to investigate the liquid film thickness and velocity distribution under different granulation operation parameters and slag physical properties. They started from the N–S equation of liquid film flow and simplified the N–S equation by the order of magnitude analysis method to obtain the liquid film thickness relationship at any radial position on the disc. Vishnu et al. [33] used a two-dimensional steady-state model to simulate the granulation process of the molten slag. They considered that the thickness of the liquid film was related to the flow rate, rotation speed, radius of rotating disc, viscosity, density of the molten slag, and surface tension. The multi-dimensional linear regression method was used to obtain the dimensionless relationship of liquid film thickness.

However, whether it is a theoretical study or a numerical simulation study, the spreading characteristics of the liquid

were often focused on the thickness of the liquid film. The influence of the outlet height of slag tube and the eccentricity between slag tube and cups on the flow characteristics of the liquid film on the surface of the rotary cup is not clear and remains to be explored by scholars.

Therefore, the authors established a three-dimensional model of centrifugal slag granulation to study the liquid film flow characteristics on the surface of the rotary cup, especially the influence of various parameters on the thickness of liquid film on the edge of the rotary cup. The influence parameters of the study included operating parameters, structural parameters of the cup, the modes of slag inlet tube and rotary cup coordination, and eccentricity. Because the thickness of the liquid film at the edge of the rotary cup is closely related to the particle size in the centrifugal granulation process, we obtained a liquid film thickness correlation at the edge of the rotary cup to predict the liquid film thickness.

Model

Governing Equation

The paper adopted a VOF model to capture the free liquid surface of the slag flowing on the surface of rotary cups. The VOF model is a flexible and effective interface tracking method based on the concept of fluid volume, which can handle arbitrary free boundary problems. The VOF model calculates the volume fraction of each phase in each control volume and combined it with the interface reconstruction method (Geo-Reconstruct) to simulate and calculate the phase interface. The volume fraction is represented as α_q . In each control unit, the sum of the volume fractions of all phases is 1. For the volume fraction α_q of the fluid in a specific unit, the value can be obtained by the following formula:

$$\alpha_q = \begin{cases} 0 & \text{no } q - \text{ phase liquid} \\ 0 \sim 1 & \text{it has an interface between } q - \text{ phase fluid and at least one phase fluid} \\ 1 & \text{filled with } q - \text{ phase fluid} \end{cases} \quad (1)$$

film were studied based on the spinning disc. For industrial practice, the granulation effect of the rotary cup is better than that of the rotating disc. Besides, in the previous studies on the spreading characteristics of molten slag liquid film, only the operating conditions (granulator speed and slag flow rate), the molten slag physical properties (temperature and viscosity), and granulator structure (diameter)

The interface between the phases is obtained by solving the continuous volume fraction equations for each phase. For the q phase, the volume ratio equation is as follows:

$$\frac{\partial \alpha_q}{\partial t} + \nabla \cdot (\mathbf{V} \alpha_q) = 0 \quad (2)$$

The physical properties in the control unit are calculated using the average volume ratio. For example, the density in each unit is given by the following formula, and other physical properties are calculated in this same way.

$$\rho = \sum \alpha_q \rho_q \tag{3}$$

The continuity equation is the following formula:

$$\frac{\partial \rho}{\partial t} + \frac{\partial(\rho u)}{\partial x} + \frac{\partial(\rho v)}{\partial y} + \frac{\partial(\rho w)}{\partial z} = 0 \tag{4}$$

The momentum conservation equation is the following formula:

$$\frac{\partial(\rho \mathbf{u})}{\partial t} + \nabla \cdot (\rho \mathbf{u} \mathbf{u}) = -\nabla p + \nabla \cdot [\mu_{\text{eff}}(\nabla \mathbf{u})] + \rho \mathbf{g} + \mathbf{F}_{SF} \tag{5}$$

The energy equation is the following formula:

$$\frac{\partial}{\partial t}(\rho E) + \nabla \cdot (\mathbf{u}(\rho E + p)) = \nabla \cdot (k_{\text{eff}} \nabla T) + S_h \tag{6}$$

The surface tension between the molten slag and air is processed into the source term in the momentum equation in the VOF model, which has the form as the following formula:

$$F_{\text{vol}} = \sigma_{ij} \frac{\rho \kappa_i \nabla \alpha_i}{\frac{1}{2}(\rho_i + \rho_j)} \tag{7}$$

In addition, the slag flow rate is a state of turbulence after calculation. With regard to the simulation study of the liquid film flow on the surface of the rotary cups and the subsequent centrifugal granulation process, the present modeling work selected the model of SST $k-\omega$ Turbulence [34]. At the same time, considering the heat transfer effect in the process of the liquid film flow, a DO radiation model and a solidification melting model were set up to analyze the heat transfer of the slag.

The DO radiation model is the discrete ordinates model. It is the most commonly used method to calculate the radiative transfer equation. The principle of this method is to calculate the ordinate component in the discrete direction. The radiation strength needs to be solved by calculating the partial differential equation on each discrete ordinate. The formula about the model can refer to the book written by the scholar, Modest Michael F [35].

For the solidification melting model, it is not necessary to trace the phase interface of the solidification and melting process. It is characterized by introducing the liquid ratio, which is the liquid volume ratio in the control volume.

$$\mu = \begin{cases} 232.82396 - 0.14543T, & 1586.15K \leq T \leq 1592.15K \\ 120.55015 - 0.13824T + 3.97397 \times 10^{-5}T^2, & 1592.15K \leq T \leq 1720.15K \end{cases} \tag{9}$$

According to the enthalpy balance, the liquid rate is calculated in each iteration. The liquid ratio is the following formula:

$$\beta = \begin{cases} 0, & T < T_{\text{solidus}} \\ \frac{T - T_{\text{solidus}}}{T_{\text{liquidus}} - T_{\text{solidus}}}, & T_{\text{solidus}} < T < T_{\text{liquidus}} \\ 1, & T > T_{\text{liquidus}} \end{cases} \tag{8}$$

Detailed meanings of the symbols used in Eqs. (1) to (8) are given in Nomenclature.

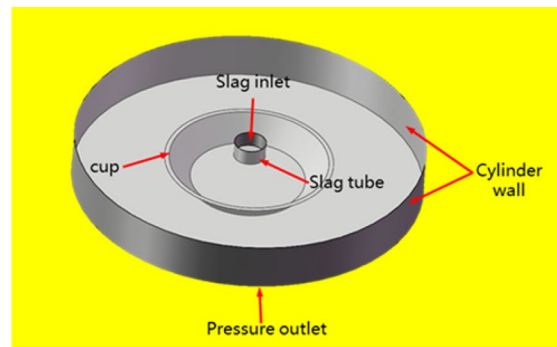
Physical Model

The centrifugal granulation process involved the stage of liquid slag outflow and granulator operation. In the actual operation process, the flow emerged fluctuation in the outflow process of liquid slag, and the granulator vibrated during operation, which caused the liquid film to be disturbed. To simplify the model, the following assumptions were adopted:

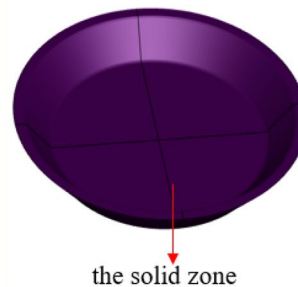
- (1) in the process of liquid film flow, the surface of the rotary cup did not consider vibration;
- (2) the mass flow at the outlet of the dropping slag tube was assumed to be constant.

A simplified three-dimensional model and the boundary conditions of the computational domain are displayed in Fig. 1. In this Fig. 1, Fig. 1a is the whole Computational domain and boundary conditions, Fig. 1b is the rotary cup which is the solid zone, and Fig. 1c is the vertical cross-sectional plot with letters from A to H. The region of space was a cylinder, where the rotary cup is located in the center of the bottom. The diameter and depth of the rotary cup were set to 50 mm and 5 mm. For the wall of the rotary cup, the inner dip angle was set to 45°. The dropping slag tube was located at the center of the top of the cylinder. For Fig. 1c, the BH is the bottom of the cylinder, which was set as the boundary condition of the pressure outlet. The CD is the slag inlet of the slag tube, which was set as the boundary of the mass flow inlet. The AB and the GH are the side of the cylinder and were set as the wall boundary condition. The AE and the FG are the top of the cylinder and were set as the wall boundary condition. The rotary cup was set as the wall boundary condition. The entire calculation domain was divided into two parts, where the large space area was set to Fluid, and the interior of the rotary cup was set to Solid. The physical parameters used in the calculation of slag and air are shown in Table 1.

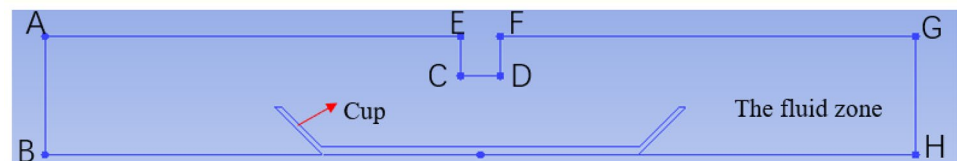
Fig. 1 Computational domain and boundary conditions



(a) The computational domain



(b) The rotary cup



(c) The boundary conditions

Table 1 Physical properties of blast furnace slag and air

Physical parameters	Unit	Slag	Air
Density	kg m ⁻³	200	1.225
Viscosity	Pa s	Formula (9)	1.7894e-05
Surface Tension	N/m	0.5[27]	

Model Verification

Grid Independence Verification

The grid generation of the computing domain including the rotary cup are shown in Fig. 2. In order to verify the reliability of the calculation model grid, for the rotary cup with a diameter of 0.05 m, we adopted, respectively, 1.35 million grids, 1.8 million grids, and 2.04 million grids to calculate the thickness of the liquid film. Moreover, the corresponding areas of the minimum grid were $3.15 \times 10^{-3} \text{ mm}^2$, $2.81 \times 10^{-3} \text{ mm}^2$, and $2.16 \times 10^{-3} \text{ mm}^2$. The results are shown in Fig. 3. The results showed that the liquid film flow

distribution from the 1.35 million grids had a particular gap comparing to the 1.8 million grids and the 2.04 million grids. However, the results of the distribution of the liquid film on the surface of the rotary cup were nearly identical for the 1.8 million and the 2.04 million grids, which are mesh independent. Therefore, in the subsequent simulations, considering the calculation accuracy and calculation amount, 1.8 million grids were selected as the simulation calculation grids.

Model Validity Verification

A rotating disc with a radius of 0.025 m to perform a corresponding numerical simulation and to obtain the liquid film thickness at the edge of the rotating disc was applied in the paper. Then the results were compared with the results of Burns et al. [36] who adopted the resistance method to measure the liquid film thickness at different positions on the surface of the rotating disc. The comparison was used to verify the accuracy of the model. The simulation conditions were the viscosity of 0.031 Pa s, the density of 1202 kg m^{-3} ,

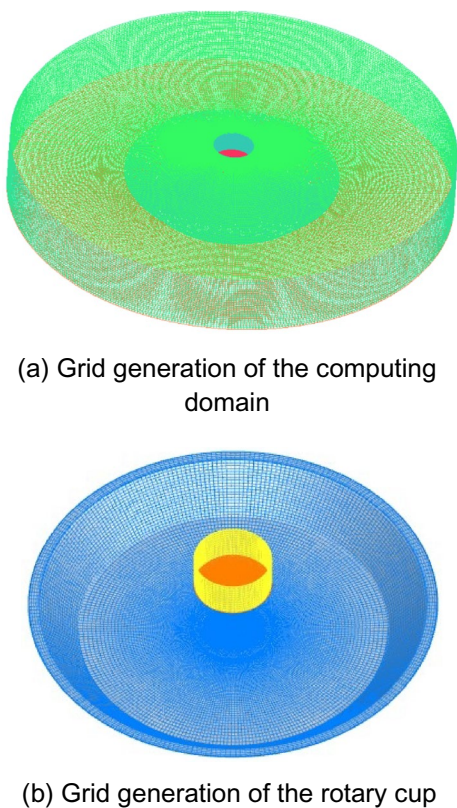


Fig. 2 Grid generation of computing domain and the rotary cup

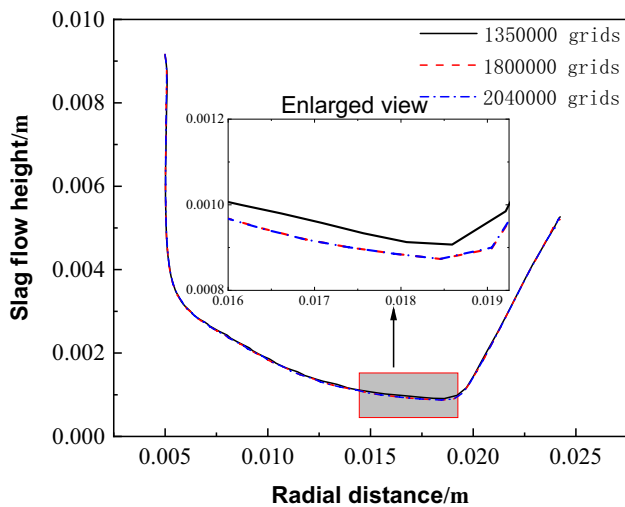


Fig. 3 Liquid film distribution on the surface of the rotary cup under different grid conditions

the speed range of 21–126 rad/s, and the flow range of $9 \times 10^{-6} \sim 17 \times 10^{-6} \text{ m}^3 \text{ s}$. The above-mentioned physical parameters are dimensionless as the following formulas.

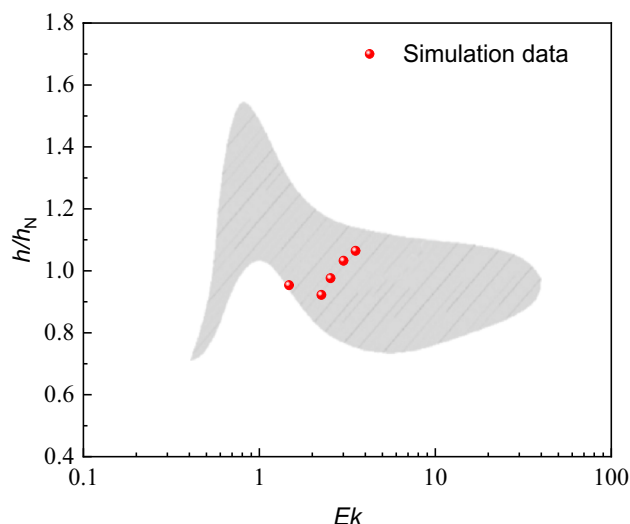


Fig. 4 Model validity verification

$$h^* = \frac{h}{h_N} \tag{10}$$

$$h_N = \left(\frac{3\mu Q}{2\pi\rho\omega^2 R^2} \right)^{1/3} \tag{11}$$

$$Ek = \left(\frac{2\pi}{3} \right)^{2/3} \left(\frac{R^4\omega\mu}{\rho Q^2} \right)^{1/3} \tag{12}$$

Detailed meanings of the symbols used in Eqs. (9) to (11) are given in Nomenclature.

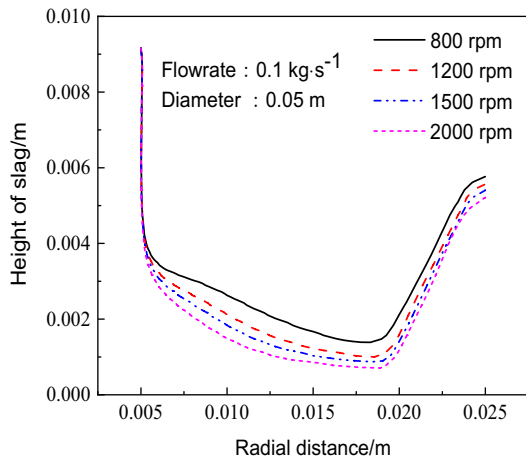
Figure 4 is a comparison between the numerical simulation results and the experimental results, where in the shaded area [36] of Fig. 4 is the thickness value of the liquid film measured in the experiment. It can be seen from Fig. 4 that the simulation results are all within the experimental area, and the simulation results have a satisfactory accuracy.

Results and Discussion

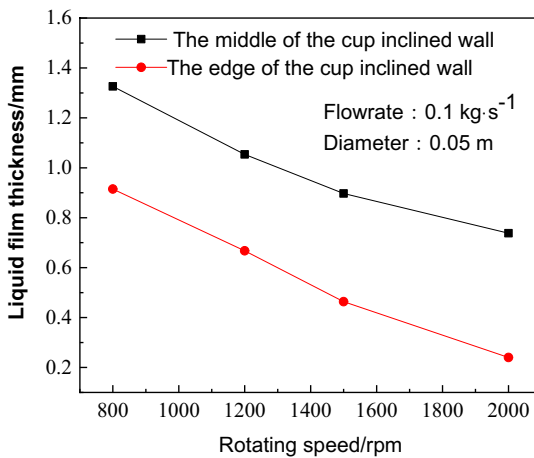
Influence of Operating Parameters on the Flow Characteristics of the Liquid Film

Influence of Rotation Speed

The liquid film distribution on the surface of the rotary cup and the thickness of the liquid film on the inclined wall of the rotary cup at different rotation speeds are described in Fig. 5. It can be seen from Fig. 5a that along the radial direction of the flat bottom of the rotary cup, the thickness



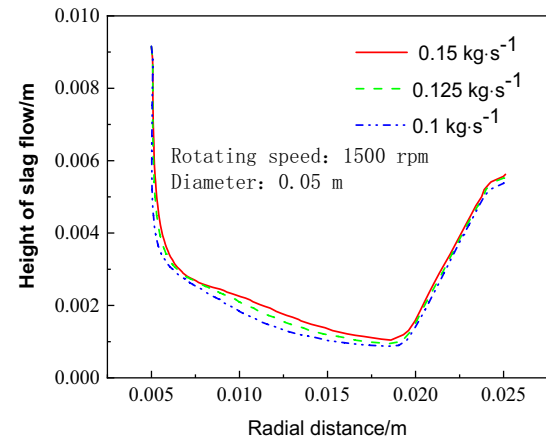
(a) Liquid film distribution at different speeds



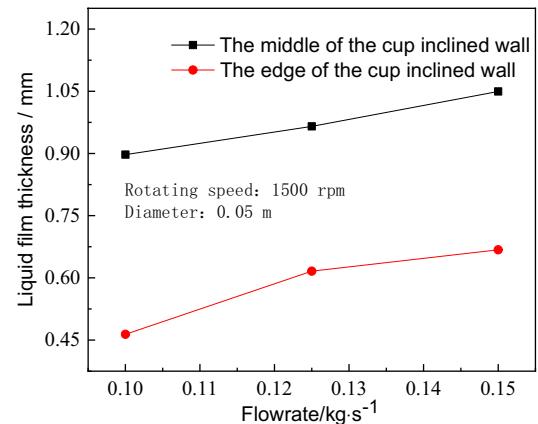
(b) Thickness of liquid film at different speeds

Fig. 5 Effect of the rotation speed of rotor on liquid film thickness

of the liquid film gradually decreased, and no hydraulic jump occurred during the entire flow process. For the rotary cup was in the radial direction of 0.015 m, when the rotation speed was 800 rpm, 1200 rpm, 1500 rpm, and 2000 rpm, the thickness of the liquid film was, respectively, 1.67 mm, 1.22 mm, 1.03 mm, and 0.86 mm. The effect of rotation speed on the liquid film thickness distribution of the entire surface was obvious. In addition, it can be seen from Fig. 5b at the half of the inclined wall of the rotary cup, the reduction rate of liquid film thickness was, respectively, about 0.00068 mm/rpm, 0.00052 mm/rpm, and 0.00032 mm/rpm when the range of the rotational speed was 800 rpm to 1200 rpm, 1200 rpm to 1500 rpm, and 1500 rpm to 2000 rpm. At the edge of the rotary cup, the reduction rate of liquid film thickness was about 0.00065 mm/rpm when the range of the rotational speed



(a) The distribution of the liquid on the surface of a rotary cup under the different flows of slag



(b) The thickness of liquid film on the inclined wall of the rotary cup under the different flow of slag

Fig. 6 Effect of slag flow rate on liquid film thickness

was 800 rpm to 1500 rpm. The reduction rate of liquid film thickness was about 0.00045 mm/rpm when the rotational speed range was 1500 rpm to 2000 rpm.

These results showed that with the increase of the rotation speed, the thickness of the liquid film on the inclined wall of the rotary cup gradually decreased, and the decreasing trend gradually became slower. The reasons are in two aspects. On the one hand, the increase of the rotational speed caused an increase of the centrifugal force, which provided the power for the radial movement of the liquid film. The increase of the radial speed promoted the decrease of the thickness of the liquid film. On the other hand, the increase of rotating speed led to the internal slip of the liquid film, and the difference between the actual radial velocity and the theoretical radial velocity

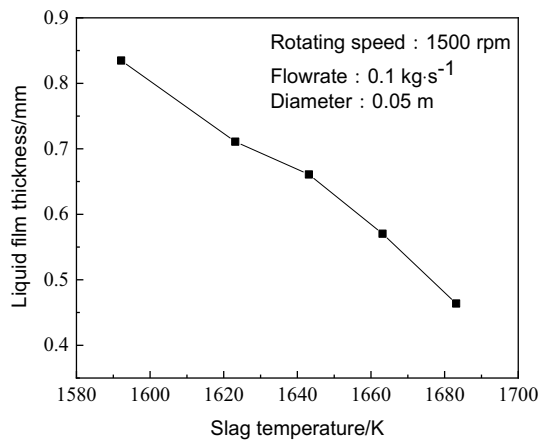


Fig. 7 Effect of different initial slag temperatures on the thickness of the liquid film at the edge of the rotary cup

increased, resulting in the decrease in the reduction of the thickness of the liquid film.

Influence of Slag Flow

Figure 6 shows the liquid film distribution on the surface of the rotary cup and the thickness distribution of the liquid film at different positions on the inclined wall surface of the rotary cup under the different slag flow rates. It can be seen from Fig. 6 that the thickness of the liquid film gradually decreased along the radial direction of the rotary cup. With the increase of slag flow rate, the thickness of liquid film on the inclined wall of the rotary cup increased gradually. At the edge of the inclined wall of the rotary cup, the flux of slag increased from 0.1 to 0.15 kg/s, and the thickness of liquid film increased from 0.46 to 0.67 mm. When the flux of slag was increased by 50%, the thickness of the liquid film was increased by 44%, which was approximately linear. This is because there was kinetic energy consumption in the impact process, which made the impact far away from the center of the rotary cup very small. Therefore, under the same other conditions, with the increase of slag flow, the thickness of the liquid film at the edge increased approximately linearly.

Influence of Slag Temperature

Figure 7 shows the effect of different slag temperatures on the thickness of the liquid film at the edge of the rotary cup. As the initial temperature of the slag decreased, the thickness of the liquid film gradually increased. When the initial temperature of the slag decreased from 1683.15 to 1643.15 K, the thickness of the liquid film increased from 0.46 to 0.66 mm. When the initial temperature of the slag further decreased to 1592.15 K, the position was called the inflection point, and the thickness of the liquid film increased to

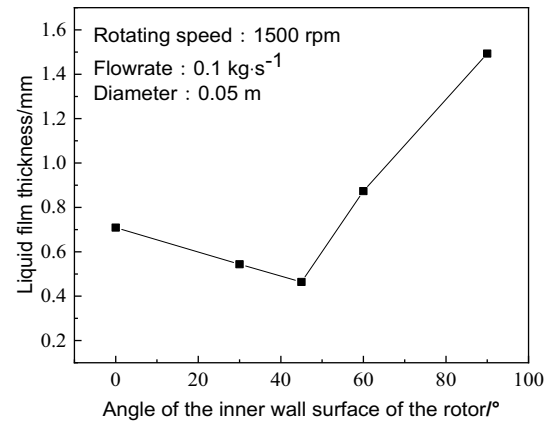


Fig. 8 Influence of the different inclination angles of the inner wall surface of the rotary cup on the thickness of the liquid film

0.84 mm. This is because as the slag's initial temperature decreased, the slag's viscosity increased, and the fluidity of the slag weakened, which caused the slag film to thicken on the surface of the rotary cup.

Influence of Rotary Cup Structure Parameters on the Flow Characteristics of the Liquid Film

Influence of the Inclination Angle of the Inner Wall Surface of the Rotary Cup

Figure 8 shows the influence of the inclination angle of the inner wall surface of the rotary cup on the thickness of the liquid film. As the inclination angle of the inner wall of the rotary cup increased, the thickness of the liquid film at the edge of the rotary cup decreased first and then increased. When the inclination angle of the inner wall surface increased from 0° to 45°, the thickness of the liquid film decreased from 0.71 to 0.46 mm, a decrease of about 34.6%. When the inclination angle of the inner wall surface increased from 45° to 90°, the thickness of the liquid film gradually increased. Especially when the inclination angle was 90°, the liquid film thickness increased to 1.49 mm. This is because the centrifugal force was perpendicular to the flow direction of the liquid film along the inclined wall of the rotary cup, which resulted in the centrifugal force not accelerating the flow of the liquid film. At the same time, the gravity acting on the liquid film was opposite to its flow direction, which hindered the movement of the liquid film along the inclined wall of the rotor and resulted in a sharp increase in the thickness of the liquid film. According to the analysis, there is an inclination angle of the inner wall of the rotary cup with the smallest liquid film thickness, which is between 30° and 60°.

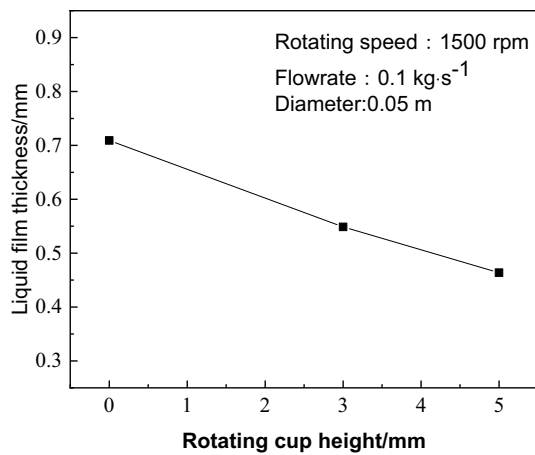


Fig. 9 Influence of the rotary cup depth on the thickness of the liquid film

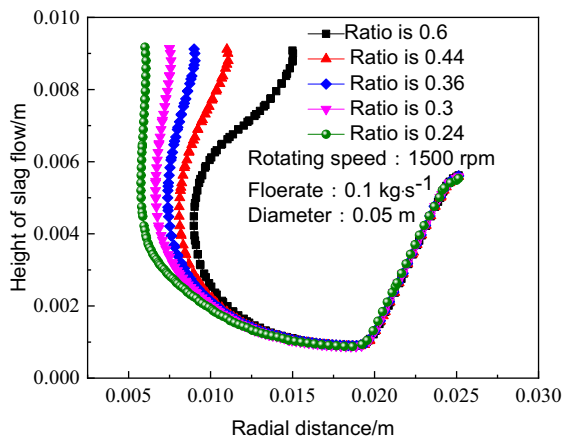


Fig. 10 Influence of the ratio of the diameter of the slag tube to the diameter of the rotary cup on the distribution of liquid film on the surface of the rotary cup

Influence of the Rotary Cup Depth

Figure 9 shows the influence of the depth of the rotary cup on the thickness of the liquid film. As the depth of the rotary cup increased, the thickness of the liquid film gradually decreased. When the depth was 0 mm, the thickness of the liquid film was 0.71 mm. As the depth was increased to 3 mm, the thickness of the liquid film at the edge of the rotary cup was reduced to 0.55 mm, a decrease of about 22.6%. When the depth of the rotor was increased to 5 mm, the thickness of the liquid film at the edge of the rotary cup was reduced to 0.46 mm, a decrease of about 15.5%. Therefore, setting the depth of the rotary cup is beneficial for thinning the liquid film. Because as the depth of the rotary cup increased, the movement time of the liquid film on the surface of the rotary cup increased, and the

spread area of the liquid film became larger, the liquid film became thinner at the edge of the rotary cup.

Influence of the Cooperating Mode of Rotating Cups and Dropping Slag Tube on the Flow Characteristics of the Liquid Film

Influence of the Ratio of the Diameter of the Slag Tube to the Diameter of the Rotary Cup

Figure 10 is the diagram of the liquid film distribution on the surface of the rotary cup under the conditions that the ratio of the diameter of the slag tube to the diameter of the rotary cup is 0.24, 0.3, 0.36, 0.44, and 0.6, respectively. When the radial distance of the rotary cup was less than 0.015 m, along the radial direction of the rotary cup, the liquid film thickness showed a decreasing trend. With the increase of the ratio, the deceleration of the liquid film thickness was larger. While when the radial distance of the rotary cup was greater than 0.015 m, although the thickness of the liquid film along the radial direction kept a decreasing trend, the film thickness tended to be uniform under the conditions of different ratios of the diameter of the slag pipe to the diameter of the rotary cup. Thus, the ratio of the diameter of the slag pipe to the diameter of the rotary cup only affected the thickness of the liquid film near the center of the rotary cup. While it was far away from the center of the rotary cup, the distribution of the thickness of the liquid film was almost not affected by the ratio.

Figure 11 shows the contour plot of the liquid film velocity on the rotor surface corresponding to the ratio of the slag tube diameter to the diameter of the rotary cup. It can be seen from Fig. 11 that the ratio only affected the liquid film flow near the center of the rotary cup, while the liquid film flow velocity far away from the center was basically the same. This is mainly because most of the energy was lost due to impact and viscous dissipation when the slag contacted with the axis of rotary cup. When the slag flowed outward along the rotary cup, the slag mainly accelerated under the action of centrifugal force. When the rotational speed was constant, the fluid obtained the same energy. Therefore, when the slag flow rate and rotating speed were constant, the slag outflow velocity decreased with the increase of the ratio of the slag tube diameter to the diameter of the rotary cup, resulting in the increase of liquid film thickness near the rotor center. But in the process of moving outward along the rotor, the flux of molten slag had little change, and the thickness of liquid film was almost the same.

Influence of the Falling Height of the Slag on the Flow Characteristics of the Liquid Film

Figure 12 shows the influence of different falling heights of the slag on the thickness of the liquid film. The greater

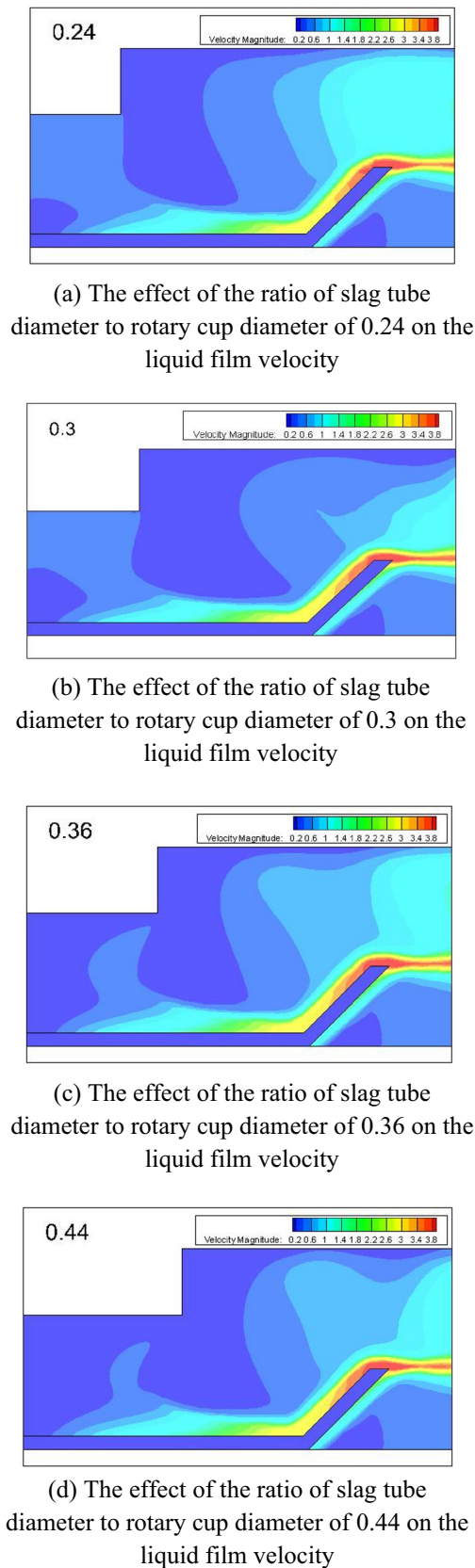


Fig. 11 Effect of the ratio of slag tube diameter to rotary cup diameter on liquid film velocity

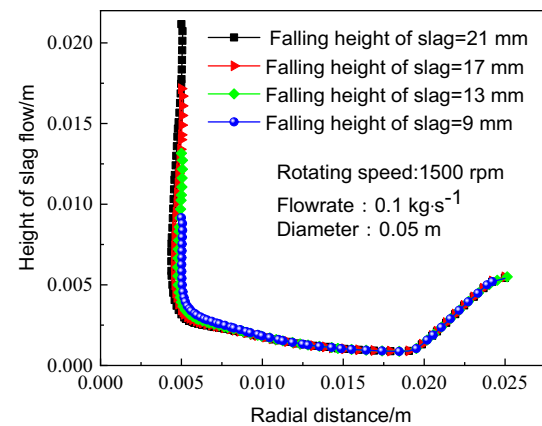


Fig. 12 Influence of different falling heights of slag on the distribution of liquid film on the surface of the rotary cup

the slag height, the smaller the cross-sectional area when the slag outflow column reached the surface of the rotary cup. When the radial distance of the rotary cup was less than 0.0125 m, along the radial direction, the difference between the liquid film thickness corresponding to the different falling heights of the slag decreased gradually. While the radial distance of the rotary cup was greater than 0.0125 m, the liquid film thickness along the radial direction still kept decreasing trend, but under the different falling heights, the liquid film thickness was almost uniform. This is because when the slag outflow and the outflow diameter were constant, as the slag height increased, the speed of the slag impacting the axis of the rotary cup increased. It caused the flow cross-sectional area to decrease when the outflow liquid column of slag reached the surface of the rotary cup. Thus, the thickness of the liquid film gradually decreased. When it was far away from the center of the rotary cup, the difference in kinetic energy caused by different slag heights was almost eliminated. The flow rate of the liquid film was basically the uniform. Therefore, the falling slag height only affected the thickness of the liquid film near the center of the rotary cup. Away from the center of the rotary cup, the liquid film thickness distribution was hardly affected by the falling height of the slag.

Influence of the Eccentricity of the Dropping Slag on the Flow Characteristics of the Liquid Film

The eccentricity distance of the dropping slag refers to the offsetting distance of the center of the dropping slag tube based on the center of the rotary cup, and its unit is mm. The eccentricity ratio of the dropping slag refers to the percentage of the eccentricity distance and the radius of the rotary cup, and its unit is %. To study the effect of slag right eccentricity on the thickness of liquid film on the rotary surface, the angle corresponding to the slag deviation direction was

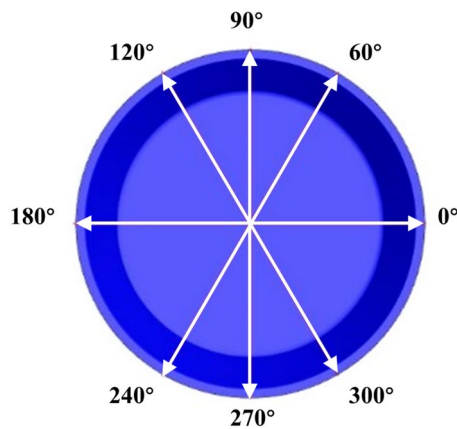


Fig. 13 Slice angle diagram of liquid film thickness in the rotary cup

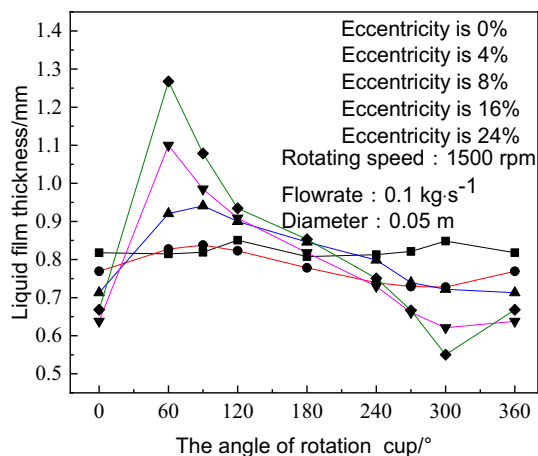


Fig. 14 Comparison of liquid film thickness at 4/5 of the inclined wall of the rotary cup under different slag right eccentricity ratios

0° and sliced along the counter clockwise circular direction. Figure 13 is the schematic diagram of the slice angle setting for the rotary cup indicating liquid film thickness.

Figure 14 shows the liquid film thickness at 4/5 of the inclined wall of the rotary cup under the different eccentricity ratios of the dropping slag. When the eccentricity ratio increased from 0 to 16%, the liquid film thickness at the 4/5 of the inclined wall of the rotary cup reduced from 0.82 to 0.64 mm, corresponding to a circumferential angle of 0°. As the eccentricity ratio increased, the liquid film thickness at the near edge of the rotary cup corresponding to the slag shift direction gradually decreased. Because as the eccentricity ratio of the falling slag increased, the degree of incomplete spread of the liquid film was higher when the liquid slag reached the inflection point on the right side of the rotary cup and the liquid was accumulated more. As the liquid migrated, the volume of the liquid moving spirally along the inclined wall near the inflection point of the rotary

cup increased, resulting in the gradual thinning of the liquid film thickness at the offset direction of the rotary cup corresponding to a circumferential angle of 0°.

In addition, along the circumferential direction, with the emergence of the eccentricity ratio of the slag, the thickness of the liquid film at the 4/5 of the inclined wall of the rotary cup generally increased first and then decreased. Taking the right eccentricity ratio of the dropping slag at 16% as an example, the liquid on the right side of the rotary cup was spirally moved upward by the centrifugal force. It caused the circumferential angle of the rotary cup to be affected from about 300°, showing an increasing trend until the liquid film thickness reached the peak value at 60° in the circumferential direction. Subsequently, due to the influence of liquid migration, the thickness of the liquid film gradually decreased in the circumferential direction until it fell to the lowest value at 300°. In general, the existence of the eccentricity ratio of the dropping slag caused two areas of the liquid film thickness near the edge of the rotary cup. Those are the area where the liquid film thickness increases gradually and the area where the liquid film thickness decreases.

At the same time, the larger the eccentricity ratio of the dropping slag, the more obvious the thickness of the liquid film at the edge of the inclined wall of the rotary cup changes along the circumferential direction. When the right eccentricity ratios were 4%, 8%, 16% and, 24%, the angles corresponding to the peaks in the area where the liquid film thickness gradually increased were 90°, 90°, 60°, and 60°, respectively. And the thickness of the liquid film at the 4/5 of the inclined wall were 0.84 mm, 0.94 mm, 1.10 mm, and 1.27 mm, which were 8.91%, 32.01%, 72.45%, and 89.66% higher than the thickness at the offset direction of the rotary cup corresponding to a circumferential angle of 0°. Compared with the slag eccentricity ratio of 0%, the thickness of the liquid film were increased by 2.30%, 14.90%, 35.04%, and 55.58%. When the right eccentricity ratio of the dropping slag was 4%, 16%, 24%, the angle corresponding to the lowest value of the gradually decreasing thickness of the liquid film was 300°. The liquid film thickness at 4/5 of the inclined wall of the rotary cup were 0.73 mm, 0.62 mm, and 0.55 mm, which were, respectively, 5.42%, 2.68%, and 17.67% smaller than the thickness of the liquid film at the offset direction of the rotary cup corresponding to a circumferential angle of 0°. Compared with the slag eccentricity of 0%, the thickness of the liquid film were reduced by 14.26%, 26.84%, and 35.16%.

Regression Analysis

The liquid film thickness of the slag at the edge of the rotary cup was mainly related to the operating parameters, the

structural parameters of the rotary cup, the physical properties of the slag, and the matching structure of the rotary cup and the dropping slag tube. The operating parameters contained the rotation speed of the rotary cup and the slag flow. The structural parameters of the rotary cup contained the radius, the inner wall inclination angle, and the depth of the rotary cup. The physical properties of the slag contained the density, viscosity, and surface tension of the slag. The matching structure of the rotary cup and the dropping slag tube contained the ratio of the diameter of the dropping slag tube to the diameter of the rotary cup and the height of the dropping tube. They can be shown by the following formula:

$$\delta = f(\omega, Q, R, \psi, h, D_L, H, \rho, \mu, \sigma) \tag{13}$$

The following formula can be obtained by the dimensional analysis of π theorem.

$$\frac{\delta}{R} = a\Pi_1^b\Pi_2^c\Pi_3^d\Pi_4^e \tag{14}$$

$$\Pi_1 = \frac{\rho \frac{(\omega^2 R \cos \psi - g \sin \psi) R}{\omega}}{\mu} = Re \tag{15}$$

$$\Pi_2 = \frac{\rho \omega^2 R^3}{\sigma} = We \tag{16}$$

$$\Pi_3 = \frac{Q_m}{\rho \omega R^3} = Q^+ \tag{17}$$

$$\Pi_4 = \frac{H}{R} \tag{18}$$

Multivariate linear fitting was performed according to the simulated data. The dimensionless correlation of the liquid film thickness obtained through dimensional analysis is as follows:

$$\frac{\delta}{R} = 2.16051 Re^{-0.65691} We^{0.14781} \left(\frac{Q_m}{\rho \omega R^3}\right)^{0.88703} \left(\frac{H}{R}\right)^{-0.26274} \tag{19}$$

The scope of application is as follows:

$$592.1762 \leq We \leq 2081.87, 0.011318 \leq Q^+ \leq 0.022635, 0.12 \leq \frac{H}{R} \leq 0.2$$

Detailed meanings of the symbols used in Eqs. (13) to (19) are given in Nomenclature.

Conclusion

In this paper, a three-dimensional model of the rotary cup was developed to simulate the spreading process of high-temperature liquid slag on the surface of the rotary cup. The flow characteristics of the liquid film on the surface of the rotary cup were analyzed and discussed with respect to the operating parameters, the structural parameters of the rotary cup, the cooperate structure of the dropping slag tube and the rotary cup, and the eccentricity. Finally, a correlation of liquid film thickness was obtained through dimensional analysis. The main conclusions obtained in this article are as follows:

- (1) The effect of the rotation speed on the thickness distribution of the liquid film on the surface of the rotary cup is obvious. As the rotation speed increased, the thickness of the liquid film on the inclined wall of the rotary cup decreased, and the decreasing trend gradually decreased.
- (2) The film thickness changed linearly with the flow rate. When the slag flow rate increased by 50%, the liquid film thickness increased by about 44%. The viscosity of slag increased with the decrease of the initial temperature of slag, which led to the spreading and thickening of liquid film on the surface of the rotary cup.
- (3) Under a given working condition, there was an inclination angle of the inner wall surface of the rotary cup corresponding to the smallest thickness of the liquid film, and the inclination angle exists between 30° and 60°. Increasing the depth from 0 to 5 mm of the rotary cup was beneficial for thinning the liquid film.
- (4) The ratio of the diameter of dropping slag tube to the diameter of the rotary cup and the dropping slag height only affects the thickness of the liquid film near the center of the rotary cup.
- (5) The existence of the eccentricity ratio of the dropping slag makes the area of gradually increasing liquid film thickness and the area of gradually decreasing the thickness of the liquid film appear along the circumference. And the larger the eccentricity ratio was, the more obvious the change of liquid film thickness along the circumference was at the edge of the inclined wall of the rotary cup.

Acknowledgements This work was supported by the National Key R&D Program of China (Grant No: 2017YFB0603604).

References

- Wang L, Sun W, Cai J, Li X (2015) Flight dynamics and sensible heat recovery of granulated blast furnace slag. *Open Fuels Energy Sci J* 8:356–360. <https://doi.org/10.2174/1876973X01508010356>
- Bisio G (1997) Energy recovery from molten slag and exploitation of the recovered energy. *Energy* 22(5):501–509. [https://doi.org/10.1016/S0360-5442\(96\)00149-1](https://doi.org/10.1016/S0360-5442(96)00149-1)
- Du B, Zhang Y (2013) Centrifugal granulation experimental study of molten blast furnace slag by rotary disk. *Energy Metall Ind* 32(4):29–32. <https://doi.org/10.3969/j.issn.1001-1617.2013.04.007>
- Zhou DD, Xu K, Zhou P, Jiang X (2020) The production of large blast furnaces of China in 2018 and thoughts of intelligent manufacturing in the ironmaking process. *Ironmak Steelmak* 47(6):650–654. <https://doi.org/10.1080/03019233.2020.1807289>
- Xu Y, Yi D, Cai Z, Liu Q, Ye H, Ye S (2007) Development of heat recovery from blast furnace slag using dry granulation methods. *China Metall* 09:1–8. <https://doi.org/10.3969/j.issn.1006-9356.2007.09.001>
- Wang H, Zhu X, Liao Q, Ding B, He XY, Tan Y (2016) Crystallization behaviors of blast furnace (BF) slag in a phase-change cooling process. *Energy Fuels* 30(4):3331–3339. <https://doi.org/10.1021/acs.energyfuels.5b03000>
- Barati M, Esfahani S, Utigard TA (2011) Energy recovery from high temperature slags. *Energy* 36(9):5440–5449. <https://doi.org/10.1016/j.energy.2011.07.007>
- Eiki K, Jun-ichiro Y, Koichi O, Taihei S, Tomohiro A (2000) Thermodynamic analysis of thermochemical recovery of high temperature wastes. *ISIJ Int* 40(3):286. <https://doi.org/10.2355/isijinternational.40.286>
- Kasai E, Kitajima T, Akiyama T, Yagi J, Saito F (1997) Rate of methane-steam reforming reaction on the surface of molten BF slag for heat recovery from molten slag by using a chemical reaction. *ISIJ Int* 37(10):1031–1036. <https://doi.org/10.2355/isijinternational.37.1031>
- Eiki K, Jun-ichiro Y, Taihei S, Tomohiro A, Vladimir K (2001) Effects of slag compositions on the rate of methane-steam reaction. *ISIJ Int* 41(2):111. <https://doi.org/10.2355/isijinternational.41.111>
- Mizuochi T, Akiyama T, Shimada T, Kasai E, Yagi J-I (2001) Feasibility of rotary cup atomizer for slag granulation. *Isij Int-ISIJ INT* 41:1423–1428. <https://doi.org/10.2355/isijinternational.41.1423>
- Pickering SJ, Hay N, Royslance TF, Thomas GH (1985) New process for dry granulation and heat recovery from molten blast-furnace slag. *Ironmak Steelmak* 12(1):14–21
- Purwanto H, Mizuochi T, Akiyama T (2005) Prediction of granulated slag properties produced from spinning disk atomizer by mathematical model. *Mater Trans* 46(6):1324–1330. <https://doi.org/10.2320/matertrans.46.1324>
- Purwanto H, Mizuochi T, Toba H, Takagi M, Akiyama T (2004) Characteristics of glass beads from molten slag produced by rotary cup atomizer. *Mater Trans* 45(12):3286–3290. <https://doi.org/10.2320/matertrans.45.3286>
- Wang H, Wu J-J, Zhu X, Liao Q, Zhao L (2016) Energy–environment–economy evaluations of commercial scale systems for blast furnace slag treatment: dry slag granulation vs. water quenching. *Appl Energy* 171:314–324. <https://doi.org/10.1016/j.apenergy.2016.03.079>
- Quader MA, Ahmed S, Ghazilla RAR, Ahmed S, Dahari M (2015) A comprehensive review on energy efficient CO₂ breakthrough technologies for sustainable green iron and steel manufacturing. *Renew Sustain Energy Rev* 50:594–614. <https://doi.org/10.1016/j.rser.2015.05.026>
- Barati M, Jahanshahi S (2020) Granulation and Heat recovery from metallurgical slags. *J Sustain Metall* 6(2):191. <https://doi.org/10.1007/s40831-019-00256-4>
- Wu J, Wang H, Zhu X, Liao Q, Li J, Lin L (2015) Characteristic of ligament in centrifugal granulation by spinning disc. *CIESC J* 66(7):2474–2480. <https://doi.org/10.11949/j.issn.0438-1157.201500008>
- Emslie AG, Bonner FT, Peck LG (1958) Flow of a viscous liquid on a rotating disk. *J Appl Phys* 29(5):858–862. <https://doi.org/10.1063/1.1723300>
- Charwat A, Kelly R, Gazley C (1972) The flow and stability of thin liquid films on a rotating disk. *J Fluid Mech* 53(2):227–255. <https://doi.org/10.1017/S0022112072000138>
- Rauscher JW, Kelly R, Cole JD (1973) An asymptotic solution for the laminar flow of a thin film on a rotating disk. *Appl Mech* 40(1):43–47. <https://doi.org/10.1115/1.3422970>
- Zhao YY (2004) Analysis of flow development in centrifugal atomization: Part I: Film thickness of a fully spreading melt. *Modell Simulat Mater Sci Eng* 12(5):959–971. <https://doi.org/10.1088/0965-0393/12/5/013>
- Zhao Y (2004) Analysis of flow development in centrifugal atomization: Part II: disintegration of a non-fully spreading melt. *Modell Simul Mater Sci Eng* 12(5):973. <https://doi.org/10.1088/0965-0393/12/5/014>
- Myers T, Charpin J (2001) The effect of the Coriolis force on axisymmetric rotating thin film flows. *Int J Non-Linear Mech* 36(4):629–635. [https://doi.org/10.1016/S0020-7462\(00\)00026-3](https://doi.org/10.1016/S0020-7462(00)00026-3)
- Pan Y, Witt P, Xie D (2010) CFD simulation of free surface flow and heat transfer of liquid slag on a spinning disc for a novel dry slag granulation process. *Progress Comput Fluid Dyn* 10:292–299. <https://doi.org/10.1504/PCFD.2010.035362>
- Pan Y, Witt P, Kuan B, Xie D (2014) CFD modelling of dry slag granulation using a novel spinning disc process, Swinburne University of Technology. <http://hdl.handle.net/1959.3/382856>
- Pan Y, Witt P, Kuan B, Xie D (2014) CFD modelling of the effects of operating parameters on the spreading of liquids on a spinning disc. *J Comput Multiphase Flows* 6(1):49–64. <https://doi.org/10.1260/1757-482X.6.1.49>
- Pan Y, Zhao M, Ma P, Li J, Huo Z, Li H (2019) CFD modeling of melt spreading behavior on spinning discs and cups for centrifugal granulation of molten slag. *J Sustain Metall* 5(2):195. <https://doi.org/10.1007/s40831-019-00213-1>
- Chang Q, Li X, Ni H, Zhu W, Pan C, Hu S (2015) Modeling on dry centrifugal granulation process of molten blast furnace slag. *ISIJ Int* 55(7):1361–1366. <https://doi.org/10.2355/isijinternational.55.1361>
- Wang D, Peng H, Ling X (2014) Ligament mode disintegration of liquid film at the rotary disk rim in waste heat recovery process of molten slag. *Energy Procedia* 61:1824–1829. <https://doi.org/10.1016/j.egypro.2014.12.222>
- Wang D, Ling X, Peng H (2015) Simulation of ligament mode breakup of molten slag by spinning disk in the dry granulation process. *Appl Therm Eng* 84:437–447. <https://doi.org/10.1016/j.applthermaleng.2015.03.003>
- Wang D, Ling X, Peng H (2014) Theoretical analysis of free-surface film flow on the rotary granulating disk in waste heat recovery process of molten slag. *Appl Therm Eng* 63(1):387–395. <https://doi.org/10.1016/j.applthermaleng.2013.11.033>
- Mantripragada VT, Sarkar S (2017) Prediction of drop size from liquid film thickness during rotary disc atomization process. *Chem Eng Sci* 158:227–233. <https://doi.org/10.1016/j.ces.2016.10.027>

34. Menter F (1993) Zonal two equation k-w turbulence models for aerodynamic flows. In: 24th Fluid dynamics conference, Orlando. doi:<https://doi.org/10.2514/6.1993-2906>
35. Modest MF (2013) Radiative heat transfer. In: Modest MF (ed) Radiative heat transfer, 3rd edn. Academic Press, Boston
36. Burns JR, Ramshaw C, Jachuck RJ (2003) Measurement of liquid film thickness and the determination of spin-up radius on a rotating disc using an electrical resistance technique. Chem Eng Sci 58(11):2245–2253. [https://doi.org/10.1016/S0009-2509\(03\)00091-5](https://doi.org/10.1016/S0009-2509(03)00091-5)

Publisher's Note Springer Nature remains neutral with regard to jurisdictional claims in published maps and institutional affiliations.

Authors and Affiliations

Ningwen Xu¹ · Jun Zhao¹ · Xi Zhang² · Meiquan Li² · Chen Ma³ · Zhiqiang Wu³ · Haiyu Meng³ · Shuzhong Wang¹ 

✉ Shuzhong Wang
18003703029@163.com

¹ Key Laboratory of Thermo-Fluid Science and Engineering, Ministry of Education, School of Energy and Power Engineering, Xi'an Jiaotong University, Xi'an 710049, People's Republic of China

² College of Engineering, Shanxi Agricultural University, Taigu 030801, People's Republic of China

³ Key Laboratory of Energy Chemical Process Intensification, School of Chemical Engineering and Technology, Xi'an Jiaotong University, Xi'an 710049, People's Republic of China